

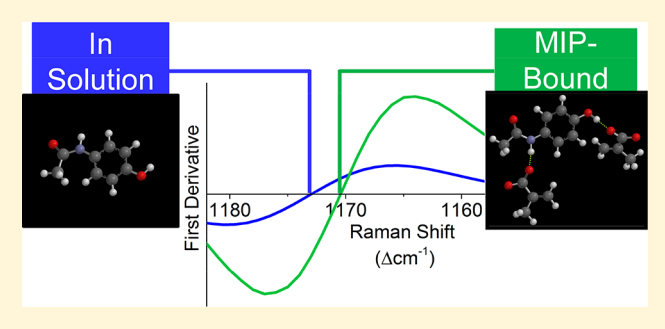
# Vibrational Frequency Shifts for Monitoring Noncovalent Interactions between Molecular Imprinted Polymers and Analgesics

Wenjing Xi, Anna A. Volkert, Michael C. Boller, and Amanda J. Haes\*

Department of Chemistry, University of Iowa, Iowa City, Iowa 52242, United States

Supporting Information

ABSTRACT: The inherent sensitivity of molecular vibrational frequencies to their local chemical environment allows for the investigation of how small molecules interact within engineered cavities in molecular imprinted polymers (MIPs). These interactions arise via weak yet collective intermolecular interaction between the polymer and small molecule. Herein, intermolecular interactions between methacrylic acid-based MIPs and acetaminophen, aspirin, and caffeine are evaluated using shifts in the vibrational frequencies and changes in bandwidths of Raman-active modes. Recognition between these materials is measured experimentally and compared to modeled



binding energies. Upon evaluation of Raman signals for the analgesics, intermolecular interactions such as hydrogen bonding and other weak interactions between the molecules and polymer backbone are quantified. Finally, dissociation constants and imprinting efficiencies are estimated for selectivity evaluation. This exploitation of the sensitivity of Raman-active vibrational band frequencies to collective intermolecular interactions for binding studies could facilitate the development and assessment of MIPs for small molecule recognition.

## **■ INTRODUCTION**

Noncovalent intra- and intermolecular interactions including hydrogen bonding as well as electrostatic,  $\pi - \pi$ , and van der Waals interactions drive rapid and reversible processes that produce metastable systems that can adapt in various pH,<sup>2</sup> ionic strengths,<sup>3</sup> pressures,<sup>4</sup> solvents,<sup>5</sup> and temperatures.<sup>6</sup> These cooperative interactions are relevant in biological mechanisms, molecular structure determination, and recognition. For example, antibody-antigen couples exhibit a combination of noncovalent interactions to promote selective binding. The energetics of these interactions can be experimentally quantified in terms of dissociation constants  $(K_d)$ , which are related to Gibbs free energies and binding energies. These quantitative values are often used to compare and contrast various binding/recognition conditions. Proteinligand interactions, for example, were characterized using surface plasmon resonance spectroscopy, and  $K_d$  values were compared to evaluate the binding affinity of analytes and varying receptors. In addition, these interactions were observed in careful surface-enhanced Raman scattering (SERS) studies where the interactions between protein receptors and bacteria were identified through shifts in vibrational features upon binding.8

Vibrational spectroscopy, in general, is a powerful tool for studying these cooperative, noncovalent intra- and intermolecular interactions in chemical systems. A variety of techniques, including infrared and Raman spectroscopies, have been used for this purpose. One compelling example of this is in understanding the effect solvation has on vibrational

frequencies for the nitrile functional group. 9,10 Vibrational modes such as C≡N symmetric stretches, which are stabilized via intermolecular interactions, red-shifted with increasing solvent polarity while isonitrile, which does not exhibit the same intermolecular interactions with solvent, was independent of solvent polarity. In another study, reduction in hydrogen bond length was shown to induce small (1-3 cm<sup>-1</sup>) but reproducible blue-shifts in vibrational frequencies associated with ionic liquids. 11 Vibrational frequencies are also sensitive to small chemical environmental changes such as phase transitions, <sup>12</sup> pressure, <sup>13</sup> and temperature. <sup>14</sup> For example, acetonitrile exhibits two stable phases:  $\alpha$  and  $\beta$ . All vibrational modes for these phases are unique including when phase transitions occur because of volume and entropy changes. 12 In all cases, vibrational frequencies have been shown to shift, 15 broaden, 15 and/or develop shoulders 16 upon changes to these chemical and physical parameters.

These same intermolecular and local environmental changes occur in both natural and artificial biological recognition couples. One engineering-based approach that has been met with modest success is noncovalent molecular imprinted polymers (MIPs) for the recognition of small molecules. 17-19 For instance, the functional monomer methacrylic acid (MAA) can be crossed linked in the presence of template molecules using ethylene glycol dimethacrylate (EGDMA) to form a

Received: August 9, 2018 Revised: September 13, 2018 Published: September 24, 2018

sorbent that contains size specific cavities with modest affinities and selectivities.  $^{18-22}$  The recognition tunability of these engineered materials has been generated for target molecules including drugs, <sup>18,23–25</sup> explosives, <sup>26</sup> enzymes, <sup>18</sup> hormones, <sup>27</sup> and sterols.<sup>28</sup> In all cases, the carboxylic acid groups in the MAA backbone can serve as either hydrogen-bond donors or acceptors, <sup>29</sup> which in combination with properly sized cavities form selective recognition sites.<sup>30</sup> The selectivity<sup>31</sup> and as a result the analytical utility of these materials to their target molecule depend on solution pH, ionic strength, and solvent as well as on the homogeneity of the polymer particle size and surface area to volume ratio.<sup>17</sup> While designing new MIPs is labor-intensive, previous studies demonstrated successful binding formulations and conditions through systematic variations in solvent composition, pH, and ionic strength.<sup>32</sup> Detection methods such as infrared spectroscopy were shown to indirectly and specifically detect target molecules using MIPs. 24,27,33,34 While these methods yielded large signals, the observed spectral signatures were typically broad and difficult to measure in aqueous environments. 35,36 Furthermore, spectral sensitivity to intermolecular interactions were not evaluated for these same reasons.

Herein, we demonstrate that Raman spectroscopy can be used to evaluate collective intra- and intermolecular interactions and/or other chemical environmental changes between noncovalent MIPs and three small analgesics including acetaminophen, aspirin, and caffeine through changes in vibrational mode frequency shifts induced at engineered binding cavities. To do so, binding energies  $(E_{\rm B})$ and intermolecular interactions that drive these interactions are modeled using density functional theory (DFT). Raman bands for acetaminophen, aspirin, and caffeine that are sensitive to intermolecular interactions and restricted motion within binding cavities are used. By evaluating the responses with respect to nonimprinted polymers, binding site densities in the MIPs, dissociation constants  $(K_d)$  of each drug-MIP complex, and drug imprinting efficiency ratios are estimated. While MIP recognition capabilities provide modest selectivity, evaluation of shifts in vibrational frequencies can be used to identify selective binding even in the presence of nonspecific binding. All in all, the combination of modest MIP selectivity and the sensitivity of vibrational band frequency variations to the local environment is expected to establish new methods for small molecule analysis.

## EXPERIMENTAL METHODS

**Materials.** Acetonitrile (C<sub>2</sub>H<sub>3</sub>N), 2-acrylamideo-2-methyl-1-propanesulfonic acid (C<sub>7</sub>H<sub>13</sub>NSO<sub>4</sub>), acetaminophen (C<sub>8</sub>H<sub>9</sub>O<sub>2</sub>N), aspirin (C<sub>11</sub>H<sub>11</sub>O<sub>6</sub>), azobisisobutylonitrile (AIBN), caffeine (C<sub>8</sub>H<sub>10</sub>N<sub>4</sub>O<sub>2</sub>), ethyl acetate (C<sub>3</sub>H<sub>8</sub>O<sub>2</sub>), ethylene glycol dimethacrylate (C<sub>10</sub>H<sub>14</sub>O<sub>4</sub>), glycidyl methacrylate (C<sub>7</sub>H<sub>10</sub>O<sub>3</sub>), 1-hydroxycyclohexyl phenyl ketone (Irgacure 184), 4-(2-hydroxyethyl)-1-piperazineethanesulfonic acid (HEPES), tetrahydrofuran (THF) (C<sub>4</sub>H<sub>8</sub>O), toluene (C<sub>7</sub>H<sub>8</sub>), and 3-trimethoxysilylpropyl acrylate (C<sub>8</sub>O<sub>8</sub>H<sub>12</sub>Si) were purchased from Sigma-Aldrich (St. Louis, MO). An over-the-counter migraine medication was purchased from a local drug store. All other chemicals were purchased from Fisher Scientific (Pittsburgh, PA). Chemicals were used as received unless otherwise stated. Water (18.2 MΩ·cm<sup>-1</sup>) was obtained using a Nanopure System from Barnstead (Dubuque, IA).

MIP Fabrication and Characterization. MIPs were prepared according to previous reports. <sup>28,37</sup> Briefly, caffeine

imprinted MIPs (MIPcaffeine) were prepared by combining and equilibrating the following for 30 min: 103  $\mu$ mol of caffeine (20 mg), 30  $\mu$ L (356  $\mu$ mol) of methacrylic acid, 235  $\mu$ L (1246 µmol) of ethylene glycol dimethacrylate, 0.7 mg of the photoinitiator Irgacure 184, 184 µL of DMSO, and 551 µL of THF. Aspirin templated methacrylate-based polymers (MI-P<sub>aspirin</sub>) were prepared by combining and equilibrating (30 min) 266  $\mu$ mol of aspirin (48 mg), 30  $\mu$ L (356  $\mu$ mol) of methacrylic acid, 235 µL of ethylene glycol dimethacrylate (1246  $\mu$ mol), 0.7 mg of Irgacure, and 735  $\mu$ L of THF. For both MIP<sub>aspirin</sub> and MIP<sub>caffeine</sub>, polymerization occurred using an OmniCure Series 1500 UV lamp with a 250-450 nm filter (P = 15 mW) for 30 min. Lyophilization of the polymers was performed using a Thermo Scientific Modulyo Freeze-Dryer for at least 24 h. Acetaminophen imprinted MIPs (MI-P<sub>acetaminophen</sub>) were prepared by combining and equilibrating (30 min) 112  $\mu$ mol (17 mg) of acetaminophen, 30  $\mu$ L (356  $\mu$ mol) of methacrylic acid, 235  $\mu$ L (1246  $\mu$ mol) of ethylene glycol dimethacrylate, 5 mg of AIBN, and 735  $\mu$ L of THF. Next, the monomer solution was purged with N<sub>2</sub>. The vials were capped and placed in a 60 °C oven for 24 h to cure. The resulting MIP<sub>acetaminophen</sub> were lyophilized for at least 24 h to remove solvent.

Drug templates were removed from the MIP via Soxhlet extraction for 8 h with dichloromethane, methanol, and ethyl acetate for caffeine, acetaminophen, and aspirin, respectively. Drug removal was confirmed using Raman difference spectra. To improve polymer uniformity, the MIPs were ground using a mortar and pestle and sieved (mesh size 707–230). The 0–63  $\mu$ m fraction was collected and used for subsequent analysis. Nonimprinted polymer standards were synthesized using identical procedures used above and previously reported literature, <sup>38</sup> except no template molecules were included.

Size analysis of fractionated MIPs was performed using DLS (Beckman Coulter DelsaNano C particle analyzer) and TEM (JEOL 1230). The MIPs were prepared for DLS by suspending 1.74 mg of the dried MIP in 10 mM NaCl in water, sonicating for  $\sim\!\!2$  min, and incubating the samples at room temperature for 30 min prior to analysis. The resulting hydrated diameters were estimated assuming a Gaussian distribution. Nonhydrated particle diameters and MIP particle morphology were imaged using TEM. These samples were prepared by suspending 0.25 mg of MIP in 50% ethanol, pipetting 10  $\mu$ L of the solution onto a carbon Formvar-coated copper grid (400 mesh, Ted Pella, Redding, CA), and air drying overnight. The resulting images were analyzed using Image Pro Analyzer, and at least 35 polymer particles were evaluated per sample to estimate dried particle dimensions.

The effective surface potential of the MIP particles was quantified using their electrophoretic mobility at 25 °C using a Malvern Zetasizer (Worcestershire, UK). The MIPs were suspended in buffer with pH ranging from 1.5 to 12. Ionic strengths were adjusted to 75 mM using a 1 M NaCl stock solution. All solutions were sonicated for ~2 min and then incubated at room temperature for 3+ h prior to analysis. The zeta potential of a material standard was used as a reference so that day-to-day measurements could be rigorously compared. Measurements were performed in triplicate, and error bars represent the standard deviation of these.

Raman Microscopy. All Raman spectra were collected using an Examiner532 Raman spectrometer (DeltaNu) mounted on an Olympus IX71 microscope equipped with a 10× objective lens and a Hamamatsu ORCA-ER camera. The

laser was focused into the polymer portion of the sample to minimize spectral contributions from the solution. Raman spectra were collected using the following parameters: excitation wavelength ( $\lambda_{ex}$ ) = 532 nm, power (P) = 8-12 mW, integration time  $(t_{int}) = 8-15$  s, and at least 10 averages. Raman intensities were collected in terms of photon counts (cts) but reported in units of cts mW<sup>-1</sup> s<sup>-1</sup> to account for slight laser power variations and integration time differences. The integrated areas of vibrational bands that are sensitive to intermolecular interactions were used for quantification. The vibrational features most sensitive to these are located at 558 cm<sup>-1</sup> (C-N-CH<sub>3</sub> deformation), 1173 cm<sup>-1</sup> (phenyl bending), and 1034 cm<sup>-1</sup> (CH<sub>3</sub> rocking) for caffeine, acetaminophen, and aspirin, respectively. Zero-point crossings of firstderivative spectra were used for determining vibrational mode frequencies. Vibrational features were also analyzed using Origin Pro 9.1 for spectral deconvolution of overlapping bands (e.g., overlap of 1037.8 cm<sup>-1</sup> (CH<sub>3</sub> rocking, aspirin) and 1044.3 cm<sup>-1</sup> (C-C stretch, polymer)) and for quantification of band widths. The vibrational band frequencies and intensities for drugs bound to the polymer were estimated using Gaussian functions. Next, vibrational band areas were divided by the Raman band areas of the polymer C-C-O stretch at 600 cm<sup>-1</sup> to account for sampling differences. Measurements were performed in triplicate, and error bars represent the standard deviation of these data.

Binding Assays. MIPs serve as hydrogen bond donors with the selected molecules when the solution pH is within  $\sim$ 1 pH unit lower than effective MIP  $pK_a$  (from the carboxylic acid in the MIP backbone). MAA polymers, however, must undergo some swelling to promote intermolecular interactions, and this only occurs if the solution pH is higher than its pK<sub>a</sub> or a swelling agent is added. 40 Thus, ideal binding conditions were optimized prior to these studies. 25 mM HEPES (pH 8.5) or 25 mM phosphate (pH 6.0) buffers were prepared with slight pH adjustments made with 1 M NaOH. Acetaminophen solutions were prepared in the HEPES buffer, and the ionic strength of the drug solutions was adjusted to 75 mM using NaCl. A 25 mM phosphate buffer (pH 6.0) was used for preparing both the caffeine and aspirin samples. This buffer was previously shown to prevent the formation of salicylic acid for aspirin. This solution was spiked with 0.3% methanol to slightly swell the polymer to promote intermolecular interactions between the analgesic and polymer. 39 All solutions were filtered using a 0.2  $\mu$ m nylon filter (Whatman, Middlesex, UK) prior to use. For Raman measurements, polymer particles were suspended in 2 mg/mL drug solutions and incubated for 12+ h. The dissociation constant and the maximum number of binding sites for each MIP were estimated using a Langmuir isotherm model (Origin Pro 9.1). Over-the-counter drug assays were performed by grinding and dissolving the pills in 25 mM HEPES buffer (pH 8.5) for the detection of acetaminophen or in 25 mM phosphate buffer (pH 6, 0.3% methanol) for aspirin and caffeine. These solutions were sonicated for 2 h, and the nonsoluble drug fillers were removed by centrifugation for 10 min at 5000g. The supernatant was collected and used for subsequent assays. Control studies were performed using nonimprinted polymers, and all experimental conditions were identical to those using MIPs.

**Imprint Site Geometries.** The imprint site volume/orientation was modeled using Spartan (Spartan '10, Version 1.1.0). Simplified binding site geometries were modeled to provide insight into intermolecular interactions between

multiple methacrylic acid monomers and either acetaminophen, aspirin, or caffeine. Calculations were performed in series starting with a Hartree–Fock 3-21G basis set, followed by DFT B3LYP 6-31G\*, DFT B3LYP 6-31+G\*, and finally DFT B3LYP 6-311+G\*\* with water as the solvent, which was simulated using the SM8 quantum mechanical aqueous continuum solvation model. Performing the calculations in series ensured that the calculations converged successfully (i.e., energy minimized and optimized binding site geometries obtained).

## ■ RESULTS AND DISCUSSION

**Promoting Site-Specific Intermolecular Interactions** between Analgesics and MIP Particles. As with any binding couple, intermolecular interactions between the polymer and target molecule depend on a combination of factors including Coulombic forces, London dispersion interactions, hydrogen bonding, and molecular properties such as polarizability and lone pair electrons. Furthermore, these intermolecular interactions between MIP particles and caffeine, acetaminophen, and aspirin depend on particle size, uniformity, and binding site accessibility. As a result, the size and surface potential of fractionated polymer particles are first evaluated as shown in Figure 1. Analysis of TEM images yields mean dehydrated MIP particle dimensions of  $421 \pm 128$  (number of particles (N) = 35),  $345 \pm 113$  (N = 51), and  $284 \pm 117$  (N = 35) nm for MIP<sub>caffeine</sub>, MIP<sub>acetaminophen</sub>, and

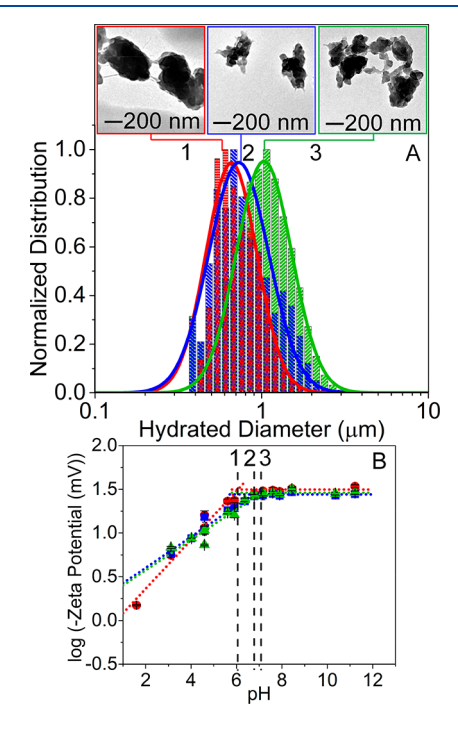


**Figure 1.** Characterization of MIPs as a function of (A) size using DLS and TEM and (B) zeta potential for (1) MIP caffeine (2) MIP acetaminophen, and (3) MIP aspirin. Lines represent Gaussian analysis; hydrated mean diameters were 740  $\pm$  200, 760  $\pm$  230, and 1140  $\pm$  350 nm for MIP caffeine, MIP acetaminophen, and MIP aspirin, respectively. The mean dimensions from TEM are 421  $\pm$  128 nm (n = 50), 345  $\pm$  113 (n = 51), and 284  $\pm$  117 (n = 35) for the same. The estimated pKa values are 6.05  $\pm$  0.43, 6.74  $\pm$  0.52, and 7.10  $\pm$  0.71 for the same. The error bars represent the standard deviation of three replicate measurements. Errors in pKa values are estimated from uncertainty in linear fittings.

MIP<sub>aspirin</sub> samples, respectively (Figure 1A). These size variations likely arise from slight differences in mechanical stability of the polymers that depend on the method of polymerization where larger particle size distributions are observed for materials synthesized using thermal polymerization (MIP<sub>acetaminophen</sub>) vs photopolymerization (MIP<sub>aspirin</sub> and MIP<sub>caffeine</sub>). While TEM provides valuable details regarding nonhydrated particle morphology, DLS reveals hydrated particle diameters that are relevant for studying intermolecular interactions. The hydrated diameters of these samples from DLS are  $740 \pm 200$ ,  $760 \pm 230$ , and  $1140 \pm 350$  nm for MIP<sub>caffeine</sub>, MIP<sub>acetaminophen</sub>, and MIP<sub>aspirin</sub>, respectively (Figure 1A). The differences in mean diameters observed between DLS and TEM are attributed to polymer swelling in aqueous environments, possible particle aggregation, and/or irregular particle morphologies. Importantly, both DLS and TEM indicate relative uniformity (RSD < 40%) among the polymer particles, and these structures can be used for subsequent binding studies and shifts in Raman frequencies.

Solution conditions (pH, ionic strength, organic additives, etc.) can also be used to promote targeted interactions between analgesics and polymer particles.<sup>43</sup> Previously, zeta potential measurements<sup>46</sup> and DFT<sup>47</sup> simulations successfully guided solvent selection for maximizing MIP-molecule interactions, 48 and the carboxylic acid/carboxylate groups in the polymer backbone were shown to govern the surface potential of the polymer particles.<sup>49</sup> As such, the log values of zeta potential are plotted as a function of pH to linearize the data (Figure 1B). As pH increases from 2 to ~7 these values increase linearly, while in more basic solutions these become approximately constant. Estimated pKa values for the carboxylate groups for each MIP occur at the intersection of these two regimes. 48 This results in carboxylate  $pK_a$  values for caffeine, acetaminophen, and aspirin MIPs of  $6.05 \pm 0.43$ , 6.74 $\pm$  0.52, and 7.10  $\pm$  0.71, respectively. These data are consistent with other reports where the  $pK_a$  of the carboxylic acid group in MAA increases from 3.5 to 4.5 in monomer form up to  $\sim$ 7.5 as the degree of polymerization increases.<sup>49</sup> Deprotonation of the carboxylic acid group becomes less favorable as polymerization increases.<sup>50</sup> We hypothesize this is related to weakening of the Lewis acidity of the functional group as polymerization occurs and/or cross-linking between linear polymers and electron density in the carboxylic acid groups increase. As a result, the  $pK_a$  depends on slight differences in polymer crosslinking. 50 This indicates that MIP<sub>aspirin</sub> is the most highly crosslinked polymer and has the lowest binding site density followed by acetaminophen and caffeine.

Because MAA-based MIPs recognize small molecules primarily through hydrogen bond formation in engineered cavities, solution pH is the most important parameter to vary to promote interactions involving the protonation state of functional groups and to minimize repulsive Coulombic interactions between the polymer and analgesics (i.e., aspirin). The molecular structures for these are shown in Figure 2A, and results from theoretical binding site predictions between the polymer and each drug molecule are shown in Figure 2B.

It should be noted that the relevant  $pK_a$  values for the three drug molecules are as follows: caffeine (-N=, 0.6), acetaminophen (-OH, 9.38), and aspirin (-COOH, 3.5). This means that each molecule should exhibit unique intermolecular interactions within the polymer cavities via hydrogen bond formation. To quantify these interactions,

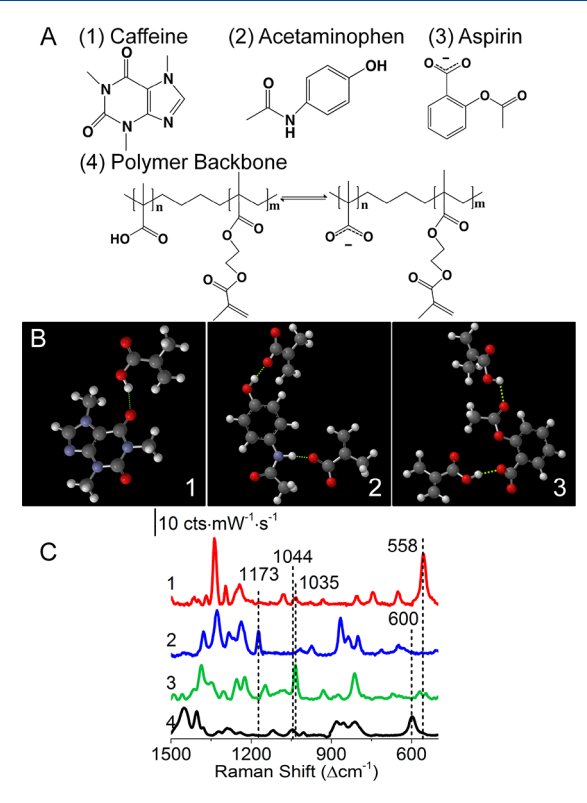


Figure 2. (A) Structures, (B) Spartan models of energy-minimized imprint geometries, and (C) Raman spectra of 90 mM (1) caffeine, (2) acetaminophen in 25 mM HEPES buffer (pH = 8.5), (3) aspirin in 25 mM phosphate buffer (pH = 6), and (4) the methacrylate polymer. The unique vibrational modes are labeled and listed in Table 2. Legend in Spartan models: red = oxygen, dark gray = carbon, light gray = hydrogen, and dotted yellow lines = hydrogen bonds. Raman parameters:  $\lambda_{\rm ex}$  = 532 nm, P = 8 mW,  $t_{\rm int}$  = 12, 6, 11, and 1 s for caffeine, acetaminophen, aspirin, and nonimprinted polymer, respectively.

binding energies  $(E_{\rm B})$  are calculated using DFT and are attained as follows:  $^{\rm S4}$ 

$$E_{\rm B} = E_{n \cdot \rm monomer + template} - E_{\rm template} - nE_{\rm monomer}$$
 (1)

where  $E_{\rm monomer}$  is the energy of polymer monomer,  $E_{\rm template}$  is the energy of drug template in its (de)protonated or neutral form,  $E_{n\cdot {\rm monomer}+{\rm template}}$  is the energy of the optimized configuration of binding sites, and n is the number of monomers that participate in hydrogen bond formation around each template molecule. Binding pockets in these noncovalent MIPs are modeled using this equation assuming that binding pockets arise from cooperative hydrogen bonding interactions between either (one or two) protonated or deprotonated monomers with the analgesics.

The results of these  $E_{\rm B}$  are summarized in Table 1, and the observed trends are consistent with previous results<sup>47</sup> that demonstrated that there are cooperative, energetically favorable effects in intermolecular interactions (i.e., increasing number of hydrogen bonds) in these systems. Several trends are noted. First, caffeine, which can undergo relatively weak hydrogen bonding between its amide functional groups and polymer (Figure 2B-1), shows the weakest binding energy relative to the other two binding couples. This result is consistent with the strength of this hydrogen bond and with previous investigations that revealed that MAA-based MIPs exhibit poor selectivity to caffeine in aqueous solutions because

Table 1. Relative Binding Energies from DFT

	DFT B3LYP6- 311+G** (hartrees)	$E_{\rm B}$ (hartrees) (from eq 1)	relative $E_{\rm B}$ (kcal/mol)
$E_{\text{monomer,1}}$ , MAA (protonated)	-306.587		
$E_{\text{monomer,2}}$ , MAA (deprotonated)	-306.133		
$E_{ m template(caffeine)} \  m (neutral)$	-680.579		
$E_{ ext{template(aspirin)}} \  ext{(negative)}$	-648.450		
$E_{ m template(acetaminophen)} \ \ \ \ \ \ \ \ \ \ \ \ \ \ \ \ \ \ \$	-515.646		
$E_{1*_{\mathrm{monomer}+caffeine}}$	-987.170	-0.005	-2.919
$E_{2*_{\mathrm{monomer}+caffeine}}$	-1293.778	-0.026	-16.241
$E_{1*_{\mathrm{monomer}+aspirin}}$	-955.074	-0.037	-23.384
$E_{2*_{\text{monomer}+aspirin}}$	-1261.698	-0.075	-47.042
$E_{1*_{\mathrm{monomer}+acetaminophen}}$	-821.784	-0.004	-2.608
$E_{2^*monomer+acetaminophen}$	-1127.952	-0.039	-24.415

of nonspecific interactions between the molecule and hydrocarbon chains from the polymer, <sup>55,56</sup> a result also consistent with our spectroscopic findings (*vide infra*).

Second, the hydroxyl group (in addition to the amide group) in acetaminophen leads to more favorable hydrogen bonding interactions to the polymer vs caffeine. A large, ~10-fold improvement in energetic favorability is estimated when both interactions are considered (Figure 2B-2). Finally, aspirin, which contains carboxylate and ester functional groups, exhibits the most energetically favorable interactions with MAA as shown in Figure 2B-3. This suggests that if the Coulombic repulsive forces between the net negatively charged polymer and net negatively charged molecule can be overcome (i.e., through swelling), the most energetically favorable intermolecular interactions should be observed between aspirin and MIP binding site cavities vs the other two engineered binding partners.

Identification of Vibrational Bands That Are Sensitive to Collective Intermolecular Interactions between the Analgesics and Polymers. Raman spectra contain narrow vibrational features that have been successfully used for detection of small molecules using MIPs.<sup>17</sup> Because we hypothesize that these modes are sensitive to cooperative intermolecular interactions, vibrational band assignments must be made before changes in these vibrational frequencies can be evaluated. To do this, Raman spectra of 90 mM (1) caffeine, (2) acetaminophen, and (3) aspirin in buffer along with the (4) methacrylate-based nonimprinted polymer are collected and analyzed (Figure 2C and Table 2). The drugs and polymer exhibit both overlapping and unique vibrational bands (complete analysis in Table S1); however, vibrational frequencies located at 558 cm<sup>-1</sup> (C-N-CH<sub>3</sub> deformation),<sup>57</sup> 1173 cm<sup>-1</sup> (phenyl bending), s8 and 1034 cm<sup>-1</sup> (CH<sub>3</sub> rocking)<sup>59</sup> for caffeine, acetaminophen, and aspirin, respectively, are selected as they participate directly in intermolecular interactions and/or exhibit restricted motion (bending modes) upon binding to three-dimensional cavities in the MIP. Importantly, because the amount of polymer present in the focal volume could change (because of polymer density variations), the Raman band associated with the methacrylate stretch at 600 cm<sup>-1</sup> is used as an internal standard as it neither changes upon polymerization nor overlaps with the selected vibrational modes. 60,61

Table 2. Unique Vibrational Frequencies ( $\Delta \overline{\nu}$ , cm<sup>-1</sup>), Full Width at Half-Maximum ( $\Gamma$ , cm<sup>-1</sup>), and Assignments for Acetaminophen, Aspirin, Caffeine, and Polymer<sup>a</sup>

molecule	in solution	with nonimprinted	MIP- bound	assignment
caffeine	558.2 ± 0.0 <sub>5</sub> , 21	$\begin{array}{c} 556.3 \pm 0.0_8, \\ 20 \end{array}$	$556.2 \pm 0.2_{0}$ , 21	$\delta$ (C-N- CH <sub>3</sub> ) <sup>57</sup>
polymer	not applicable	$600 \pm 1, 26$	$600 \pm 1,$ $27$	ν(C–C– Ο) <sup>60</sup>
aspirin	$1034.7 \pm 0.0_{5}$ , 14	1034.9 ± 0.4 <sub>0</sub> , 16	$1037.8 \pm 0.2_{2}$ 19	r(CH <sub>3</sub> ) <sup>59</sup>
polymer	not applicable	$1043.6 \pm 0.2_7, 23$	$1044.4 \pm 0.4_3, 21$	$\nu$ (C–C) <sup>62</sup>
acetaminophen	1173.0 ± 0.0 <sub>3</sub> , 15	1171.9 ± 0.1 <sub>0</sub> , 14	$1170.7 \pm 0.2_6, 16$	$\beta$ (phenyl) <sup>58</sup>

<sup>&</sup>quot;Average  $\pm$  standard deviations from three replicate measurements. Abbreviations:  $\delta$  = deformation;  $\nu$  = stretching; R = rocking;  $\beta$  = inplane bending.

To evaluate both specific and nonspecific interactions between the polymer and small molecules, Raman microscopy is used. Collective intermolecular interactions between the analgesics and MIP are expected to be energetically more favorable and exhibit a greater influence on vibrational band features than those nonspecifically or weakly adsorbed to the surfaces of the polymer particles. As such, vibrational frequency and bandwidth changes for the three drug molecules are evaluated upon incubation in their respective MIP and nonimprinted polymer. Changes in these spectral features are reported with respect to values collected in solution to evaluate molecules in the binding pockets (cooperative intermolecular interactions) or at the polymer surface (nonspecific, relatively weaker interactions).

Representative spectra and first-derivative spectra for each drug in solution as well as with both nonimprinted and molecular imprinted polymers are shown in Figure 3. Because shifts in vibrational frequency upon changes in local intermolecular interactions are small, 63 first-derivative spectra allow for these small changes to be easily observed. Results of this analysis as well as changes in vibrational band widths are summarized in Table 2. Two general trends are observed. First, the vibration bandwidths for acetaminophen and aspirin increase 2-5 cm<sup>-1</sup> when specifically bound to the MIP vs in solution or nonspecifically interacting with the polymer. These variations are consistent with similar line width increases observed when comparing normal Raman scattering to SERS spectral features.<sup>64</sup> For instance, the CH<sub>3</sub> rocking vibrational mode in aspirin broadens from 14 to 19 cm<sup>-1</sup> in width upon binding to the MIP vs in solution. Previously, similar line broadening was attributed to an increase in compressive stress<sup>65</sup> and lifetime broadening. <sup>66</sup> Because vibrational motion is restricted upon binding in the engineered MIP cavities, the excited-state lifetime should decrease upon interaction with the polymer backbone. Similar trends are observed for most vibrational modes for acetaminophen and aspirin while only slight variations are observed for caffeine modes.

Second, some of the selected vibrational modes either redor blue-shift upon MIP binding vs in solution or via nonspecific interactions, thus indicating the nature of the collective intermolecular interactions between the analgesics and polymers. Similar results induced from hydrogen bonding, \$4,67-70 bond lengthening, \$42,54,71 and/or increased

The Journal of Physical Chemistry C

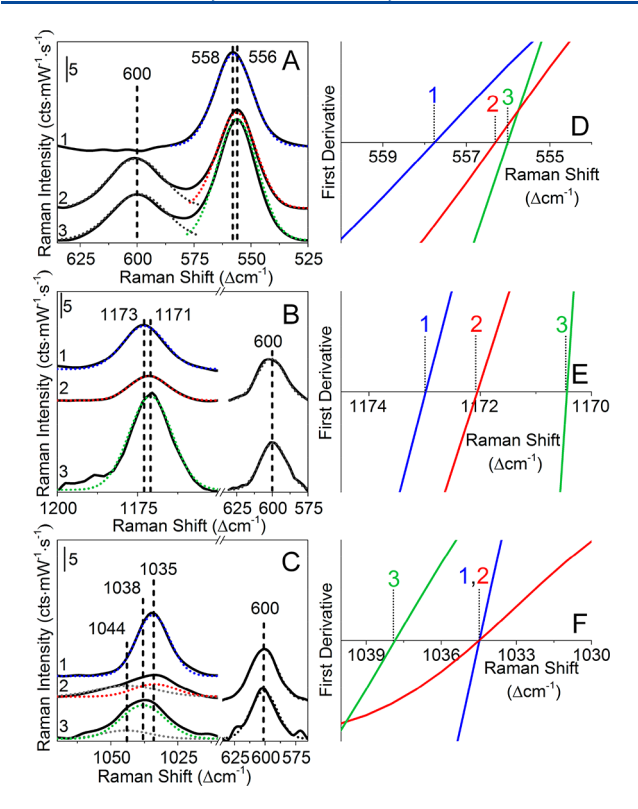


Figure 3. Representative Raman spectra and corresponding firstderivative spectra for 90 mM (A, D) caffeine, (B, E) acetaminophen, and (C, F) aspirin (1) in solution, (2) nonimprinted polymer, and (3) MIP. To collect these measurements, 2 mg/mL drug solutions were incubated with 10-20 mg polymer for 12+h. Unique vibrational mode frequencies are determined from the zero-point crossing of the first-derivative spectra. Gaussian function analysis (green, red, and gray dotted lines) are included to represent drug bound to the MIP, drug bound to the nonimprinted polymer, and polymer features, respectively. Spectra are offset for clarity. Raman parameters:  $\lambda_{\rm ex}$  = 532 nm, P = 8-12 mW,  $t_{int} = 12$ , 6, and 11 s for caffeine, acetaminophen, and aspirin in solution and 8-15 s for drugs with polymer.

pressure and/or van der Waals/London dispersion interactions  $^{65,72}$  are observed. For instance, the C-N-CH<sub>3</sub> mode associated with caffeine red-shifts from 558 cm<sup>-1</sup> in buffer to 556 cm<sup>-1</sup> when bound to the MIP (Figure 3A,D). A similar response to the solution value is observed when caffeine is incubated with a nonimprinted polymer indicating this response likely arises from nonspecific interactions, through weak hydrogen bond formation, and/or from caffeine binding to the surface of the polymer rather than the targeted binding sites. As summarized in Table S1, most vibrational modes for caffeine do not shift or exhibit small shifts from solution to the nonimprinted or molecular imprinted polymers. This result is expected, as discussed, given the nature of the predicted weak hydrogen bond and the apolar interactions that give rise to nonspecific interactions for caffeine and this MIP.<sup>5</sup>

This response represents a worst-case scenario, and one that can be improved upon with collective and stronger intermolecular interactions. Acetaminophen shows a 2 cm<sup>-1</sup> red-shift in its in-plane phenyl bending mode (1171-1173 cm<sup>-1</sup>) upon binding to the MIP vs solution. This vibrational frequency shift is twice as large as when the assay is performed with the nonimprinted polymer. While small but reasonable given the nature of the association, this suggests that the amide

group in acetaminophen participates in hydrogen bonding to the polymer backbone as modeled in Figure 2B-2. With the exception of C=C modes, similar ~1-3 cm<sup>-1</sup> vibrational frequency shifts are observed for most modes associated with acetaminophen incubated MIP (vs the nonimprinted polymer), thus further supporting that collective intermolecular interactions are being detected (Table S1).

The largest collective intermolecular interactions and sitespecific binding is observed for aspirin. As shown in Figures 3C,F, the CH<sub>3</sub> rocking mode blue-shifts from 1035 to 1038 cm<sup>-1</sup> upon incubation with the MIP. This mode, which does not directly undergo hydrogen bonding with the polymer, is restricted when bound in a site-specific cavity in the MIP causing this frequency to increase. This is further confirmed as this vibrational frequency does not shift upon incubation with the nonimprinted polymer. A similar trend is observed when comparing the vibrational frequency of this band in solution vs solid state, 73 thus confirming our assertion that vibrational frequencies are sensitive to collective intermolecular interactions.

Quantifying Intermolecular Interactions between the Analgesics and Polymer. Building on the premise that vibrational frequencies associated with the molecules are sensitive to collective intermolecular interactions, the strength of these interactions can be quantified. To do this, varying concentrations of each molecule are incubated with both its molecular and nonimprinted polymer. First, complete calibration curves for all three drugs are shown in Figure S1 while difference spectra for varying analgesic concentrations and the respective MIP-drug complexes are found in Figure S2. To correct for the nonspecific interactions and varying Raman cross sections for the selected modes/binding site densities (see Figure S3), the nonimprinted polymer responses are subtracted from the specific responses and normalized to the cross section of the band used for caffeine. These data are summarized in Figure 4A and reveal that the Raman signals increase with increasing concentration until saturation of the binding sites occurs.

To quantify differences between each binding couple and their unique intermolecular interactions, Langmuir 74,75 and Freundlich-Langmuir adsorption isotherms 76 are considered so that  $K_d$  and binding site concentrations in the MIP for the small molecule can be determined. The equilibrium binding model describes the drug-MIP interaction as follows: 77,78

$$\mathrm{drug} + \mathrm{MIP} \rightleftharpoons \mathrm{drug} - \mathrm{MIP} \quad \text{where } K_{\mathrm{d}} = \frac{[\mathrm{MIP}][\mathrm{drug}]}{[\mathrm{drug} - \mathrm{MIP}]}$$

where  $K_d$  is assumed to be dependent on hydrogen bonding and other collective intermolecular interactions.<sup>79</sup> The adsorption capacity  $(Q_m)^{54}$  is then calculated using equilibrium concentrations  $(C_e)$  as follows:

$$Q_{\rm e} = \frac{Q_{\rm m}C_{\rm e}}{K_{\rm d} + C_{\rm e}} \tag{3}$$

Several trends are noted. The  $K_d$  for the respective drugs with MIP<sub>caffeine</sub>, MIP<sub>acetaminophen</sub>, and MIP<sub>aspirin</sub> are estimated to be  $126 \pm 44$ ,  $46 \pm 6$ , and  $31 \pm 12$  mM, respectively, as summarized in Table 3. The values for acetaminophen and aspirin fall within the range of previously reported for MAAbased MIPs, which ranged from  $1 \times 10^{-3}$  to 50 mM. <sup>80,81</sup> The largest  $K_d$  is observed for caffeine, a response consistent with

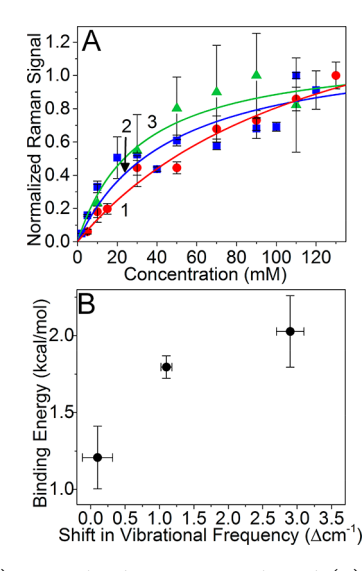


**Figure 4.** (A) Normalized Raman signals and (B) binding energy analysis for each MIP relative to the nonimprinted polymer response for (1) caffeine ( $K_{\rm d}=126\pm44$  mM,  $E_{\rm B}=1.21\pm0.20$  kcal/mol), (2) acetaminophen ( $K_{\rm d}=46\pm6$  mM,  $E_{\rm B}=1.80\pm0.07$  kcal/mol kcal/mol), and (3) aspirin ( $K_{\rm d}=31\pm12$  mM,  $E_{\rm B}=2.03\pm0.23$  kcal/mol). Lines represent Langmuir isotherm analysis. When relevant, the fit analysis for the nonimprinted polymer data was used for determining these responses.

intermolecular interaction modeling results and indicators of nonspecific interactions in vibrational frequency shift analysis. Most importantly, these values are related to Gibbs free energies ( $\Delta G = -RT \ln(1/K_{\rm d})$  and  $E_{\rm B}$ . Binding energies for the three molecules and their MIPs are compared in Figure 4B and related to shifts in their vibrational frequencies upon binding. The weak collective intermolecular interactions observed between aspirin and its MIP result in a binding energy of ~2 kcal/mol. As these interactions weaken as observed in acetaminophen and then caffeine, this vibrational frequency shift and associated binding energies similarly decrease.

To assess the significance of these binding energies, a selectivity assay is performed using a commercial migraine medication that contains caffeine, acetaminophen, and aspirin and their respective molecular and nonimprinted polymers. A selectivity value, which is defined as the ratio between an imprinting efficiency ratio between the targeted and nontargeted guest molecule responses, is calculated for each MIP. For MIP caffeine, these are  $1.3 \pm 0.2$  and  $1.2 \pm 0.2$  for the nontargeted molecules of acetaminophen and aspirin, respectively; for MIP acetaminophen,  $1.8 \pm 0.2$  when the nontargeted guest molecule is caffeine (note that aspirin exhibited no interactions with the polymer because of Coulombic repulsions so was not included); and for MIP aspirin,  $2.97 \pm 0.74$ 

and 2.49  $\pm$  0.87 when the nontarget guest molecules are acetaminophen and caffeine, respectively. These values are consistent with other MAA MIPs <sup>55,82</sup> and to our estimated binding energies. MIP<sub>caffeine</sub> shows the lowest selectivity because of the previously discussed nonspecific intermolecular interactions to the polymer. Furthermore, MIP<sub>aspirin</sub> exhibited more selectivity for acetaminophen than for caffeine, a result arising from acetaminophen and aspirin exhibiting similar sizes in the molecular imprinted polymer binding pockets.

## CONCLUSIONS

In summary, the inherent sensitivity of Raman vibrational mode frequencies to the chemical environment allowed for identification and quantification of collective noncovalent intermolecular interactions between three analgesics and molecular imprinted polymers. Building on previous work where up to a 3 cm<sup>-1</sup> shift in vibrational frequency was used to detect similar interactions, shifts in vibrational frequencies associated with the molecules were compared between solution and with both their molecular imprinted and nonimprinted polymers. While hydrogen bond formation was the dominating intermolecular interaction that drove recognition at binding sites, each molecule and its engineered polymer exhibited unique binding energies and selectivities. These binding energies correlated directly with shifts in vibrational frequency. Larger frequency shifts were observed when each analgesic was incubated in their molecular imprinted polymers compared to control polymers, indicating larger affinities to the binding sites as well as higher polymer selectivity to the targeted analgesic. All in all, this suggests that shifts in Raman vibrational frequencies can be used to evaluate the collective intermolecular interactions between engineered MIPs and small molecules, thus providing a direct method for the specific detection of analytes even in the presence of other competing nonspecific interactions.

## ASSOCIATED CONTENT

## S Supporting Information

The Supporting Information is available free of charge on the ACS Publications website at DOI: 10.1021/acs.jpcc.8b07771.

Raman band assignments, calibration curves for caffeine, acetaminophen, and aspirin, accounting for nonspecific responses of analgesics to the polymer (PDF)

# AUTHOR INFORMATION

## **Corresponding Author**

\*(A.J.H.) E-mail amanda-haes@uiowa.edu; Ph (319) 384-3695; Fax (319) 335-1270.

Table 3. Summary of Averages ( $\pm$  Standard deviations) in Vibrational Frequency Shifts from Solution to MIP or to Nonimprinted Polymer, Dissociation Constants ( $K_d$ , mM), Imprinting Efficiency Ratios, and Maximum Binding Capacities (Three Replicate Measurements Were Used)

						$max\ binding\ sites\ (binding\ sites/g\ of\ hydrated\ polymer)$		
molecule	shift in $\overline{\nu}$ to MIP $(\Delta \text{cm}^{-1})$	$K_{\rm d}~({\rm mM})$	shift in $\overline{ u}$ to nonimprinted $(\Delta \mathrm{cm}^{-1})$	imprinting efficiency	max binding capacity (mM)	theor	exptl	%
caffeine	$2.2 (\pm 0.2_0)$	126 (±44)	$2.1 (\pm 0.0_9)$	1.3 (±0.4)	27.5 (±5.1)	$2.23 \times 10^{20}$	$4.52 \ (\pm 0.85) \times 10^{19}$	20.3 (±3.8)
aspirin	$3.1 (\pm 0.2_2)$	31 (±12)	$0.2 (\pm 0.4_0)$	2.1 (±1.9)	19.0 $(\pm 6.5)$	$5.77 \times 10^{20}$	$3.12 (\pm 1.08) \times 10^{19}$	5.4 (±1.9)
acetaminophen	$2.3 (\pm 0.2_6)$	46 (±6)	$1.2 \ (\pm 0.1_0)$	4.6 (±0.9)	109.9 (±9.1)	$2.40 \times 10^{20}$	$18.08 \ (\pm 1.49) \times 10^{19}$	75.4 (±4.5)

## ORCID ®

Wenjing Xi: 0000-0003-1284-2056 Amanda J. Haes: 0000-0001-7232-6825

## **Present Addresses**

A.A.V.: Department of Chemistry, Gustavus Adolphus College, Saint Peter, MN 56082.

M.C.B.: College of Pharmacy, University of Iowa, Iowa City, IA 52242.

#### **Notes**

The authors declare no competing financial interest.

#### ACKNOWLEDGMENTS

Research reported in this publication was supported by the National Science Foundation (CHE-1707859 and CHE-1150135).

## REFERENCES

- (1) Frieden, E. Non-Covalent Interactions: Key to Biological Flexibility and Specificity. J. Chem. Educ. 1975, 52, 754-761.
- (2) Schmaljohann, D. Thermo- and pH-Responsive Polymers in Drug Delivery. Adv. Drug Delivery Rev. 2006, 58, 1655-1670.
- (3) Mianehrow, H.; Moghadam, M. H. M.; Sharif, F.; Mazinani, S. Graphene-Oxide Stabilization in Electrolyte Solutions Using Hydroxyethyl Cellulose for Drug Delivery Application. Int. J. Pharm. 2015, 484, 276-282,
- (4) Boonyaratanakornkit, B. B.; Park, C. B.; Clark, D. S. Pressure Effects on Intra- and Intermolecular Interactions within Proteins. Biochim. Biophys. Acta, Protein Struct. Mol. Enzymol. 2002, 1595, 235-
- (5) Barratt, E.; Bingham, R. J.; Warner, D. J.; Laughton, C. A.; Phillips, S. E. V.; Homans, S. W. van der Waals Interactions Dominate Ligand-Protein Association in a Protein Binding Site Occluded from Solvent Water. J. Am. Chem. Soc. 2005, 127, 11827-11834.
- (6) Jiménez Riobóo, R. J.; Philipp, M.; Ramos, M. A.; Krüger, J. K. Concentration and Temperature Dependence of the Refractive Index of Ethanol-Water Mixtures: Influence of Intermolecular Interactions. Eur. Phys. J. E: Soft Matter Biol. Phys. 2009, 30, 19-26.
- (7) Patching, S. G. Surface Plasmon Resonance Spectroscopy for Characterisation of Membrane Protein-Ligand Interactions and Its Potential for Drug Discovery. Biochim. Biophys. Acta, Biomembr. 2014, 1838, 43-55.
- (8) Costas, C.; López-Puente, V.; Bodelón, G.; González-Bello, C.; Pérez-Juste, J.; Pastoriza-Santos, I.; Liz-Marzán, L. M. Using Surface Enhanced Raman Scattering to Analyze the Interactions of Protein Receptors with Bacterial Quorum Sensing Modulators. ACS Nano **2015**, 9, 5567-5576.
- (9) Błasiak, B.; Londergan, C. H.; Webb, L. J.; Cho, M. Vibrational Probes: From Small Molecule Solvatochromism Theory and Experiments to Applications in Complex Systems. Acc. Chem. Res. 2017, 50, 968-976.
- (10) Blasiak, B.; Ritchie, A. W.; Webb, L. J.; Cho, M. Vibrational Solvatochromism of Nitrile Infrared Probes: Beyond the Vibrational Stark Dipole Approach. Phys. Chem. Chem. Phys. 2016, 18, 18094-
- (11) Fumino, K.; Wulf, A.; Ludwig, R. The Cation-Anion Interaction in Ionic Liquids Probed by Far-Infrared Spectroscopy. Angew. Chem., Int. Ed. 2008, 47, 3830-3834.
- (12) Abramczyk, H.; Paradowska-Moszkowska, K. The Correlation between the Phase Transitions and Vibrational Properties by Raman Spectroscopy: Liquid-Solid  $\beta$  and Solid  $\beta$ -Solid  $\alpha$  Acetonitrile Transitions. Chem. Phys. 2001, 265, 177-191.
- (13) Schindler, W.; Sharko, P.; Jonas, J. Raman Study of Pressure Effects on Frequencies and Isotropic Line Shapes in Liquid Acetone. J. Chem. Phys. 1982, 76, 3493-3496.
- (14) Huang, W.; Frech, R. Vibrational Spectroscopic and Electrochemical Studies of the Low and High Temperature Phases of

- $LiCo_{1-X}$  MXO<sub>2</sub> (M = Ni or Ti). Solid State Ionics **1996**, 86–88, 395–
- (15) DeVetter, B. M.; Mukherjee, P.; Murphy, C. J.; Bhargava, R. Measuring Binding Kinetics of Aromatic Thiolated Molecules with Nanoparticles Via Surface-Enhanced Raman Spectroscopy. Nanoscale 2015, 7, 8766-8775.
- (16) Kitt, J. P.; Bryce, D. A.; Minteer, S. D.; Harris, J. M. Raman Spectroscopy Reveals Selective Interactions of Cytochrome C with Cardiolipin That Correlate with Membrane Permeability. J. Am. Chem. Soc. 2017, 139, 3851-3860.
- (17) Volkert, A. A.; Haes, A. J. Advancements in Nanosensors Using Plastic Antibodies. Analyst 2014, 139, 21-31.
- (18) Haupt, K.; Mosbach, K. Molecularly Imprinted Polymers and Their Use in Biomimetic Sensors. Chem. Rev. 2000, 100, 2495-2504.
- (19) Wulff, G. Enzyme-Like Catalysis by Molecularly Imprinted Polymers. Chem. Rev. 2002, 102, 1-28.
- (20) Piletsky, S. A.; Matuschewski, H.; Schedler, U.; Wilpert, A.; Piletska, E. V.; Thiele, T. A.; Ulbricht, M. Surface Functionalization of Porous Polypropylene Membranes with Molecularly Imprinted Polymers by Photograft Copolymerization in Water. Macromolecules 2000, 33, 3092-3098.
- (21) Xie, C.; Liu, B.; Wang, Z.; Gao, D.; Guan, G.; Zhang, Z. Molecular Imprinting at Walls of Silica Nanotubes for Tnt Recognition. Anal. Chem. 2008, 80, 437-443.
- (22) Piletsky, S. A.; Piletskaya, E. V.; Sergeyeva, T. A.; Panasyuk, T. L.; El'skaya, A. V. Molecularly Imprinted Self-Assembled Films with Specificity to Cholesterol. Sens. Actuators, B 1999, 60, 216-220.
- (23) Nematollahzadeh, A.; Shojaei, A.; Abdekhodaie, M. J.; Sellergren, B. Molecularly Imprinted Polydopamine Nano-Layer on the Pore Surface of Porous Particles for Protein Capture in HPLC Column. J. Colloid Interface Sci. 2013, 404, 117-126.
- (24) Lasáková, M.; Thiébaut, D.; Jandera, P.; Pichon, V. Molecularly Imprinted Polymer for Solid-Phase Extraction of Ephedrine and Analogs from Human Plasma. J. Sep. Sci. 2009, 32, 1036-1042.
- (25) González, G.; Hernando, P.; Durand Alegría, J. A Mip-Based Flow-through Fluoroimmunosensor as an Alternative to Immunosensors for the Determination of Digoxin in Serum Samples. Anal. Bioanal. Chem. 2009, 394, 963-970.
- (26) Stringer, R. C.; Gangopadhyay, S.; Grant, S. A. Detection of Nitroaromatic Explosives Using a Fluorescent-Labeled Imprinted Polymer. Anal. Chem. 2010, 82, 4015-4019.
- (27) Tse Sum Bui, B.; Merlier, F.; Haupt, K. Toward the Use of a Molecularly Imprinted Polymer in Doping Analysis: Selective Preconcentration and Analysis of Testosterone and Epitestosterone in Human Urine. Anal. Chem. 2010, 82, 4420-4427.
- (28) Spizzirri, U. G.; Peppas, N. A. Structural Analysis and Diffusional Behavior of Molecularly Imprinted Polymer Networks for Cholesterol Recognition. Chem. Mater. 2005, 17, 6719-6727.
- (29) Suárez-Rodríguez, J. L.; Díaz-García, M. E. Flavonol Fluorescent Flow-through Sensing Based on a Molecular Imprinted Polymer. Anal. Chim. Acta 2000, 405, 67-76.
- (30) Hwang, C.-C.; Lee, W.-C. Chromatographic Characteristics of Cholesterol-Imprinted Polymers Prepared by Covalent and Non-Covalent Imprinting Methods. J. Chromatogr. A 2002, 962, 69-78.
- (31) Kantarovich, K.; Tsarfati, I.; Gheber, L. A.; Haupt, K.; Bar, I. Writing Droplets of Molecularly Imprinted Polymers by Nano Fountain Pen and Detecting Their Molecular Interactions by Surface-Enhanced Raman Scattering. Anal. Chem. 2009, 81, 5686-
- (32) Vasapollo, G.; Sole, R. D.; Mergola, L.; Lazzoi, M. R.; Scardino, A.; Scorrano, S.; Mele, G. Molecularly Imprinted Polymers: Present and Future Prospective. Int. J. Mol. Sci. 2011, 12, 5908-5945.
- (33) Tov, O. Y.; Luvitch, S.; Bianco-Peled, H. Molecularly Imprinted Hydrogel Displaying Reduced Non-Specific Binding and Improved Protein Recognition. J. Sep. Sci. 2010, 33, 1673-1681.
- (34) Kong, Q.; Wang, Y.; Zhang, L.; Ge, S.; Yu, J. A Novel Microfluidic Paper-Based Colorimetric Sensor Based on Molecularly Imprinted Polymer Membranes for Highly Selective and Sensitive Detection of Bisphenol A. Sens. Actuators, B 2017, 243, 130-136.

- (35) Jakusch, M.; Janotta, M.; Mizaikoff, B.; Mosbach, K.; Haupt, K. Molecularly Imprinted Polymers and Infrared Evanescent Wave Spectroscopy. A Chemical Sensors Approach. *Anal. Chem.* **1999**, *71*, 4786–4791.
- (36) Liu, W.; Li, H.; Yu, S.; Zhang, J.; Zheng, W.; Niu, L.; Li, G. Poly(3,6-Diamino-9-Ethylcarbazole) Based Molecularly Imprinted Polymer Sensor for Ultra-Sensitive and Selective Detection of  $17-\beta$ -Estradiol in Biological Fluids. *Biosens. Bioelectron.* **2018**, 104, 79–86.
- (37) Rosengren-Holmberg, J. P.; Karlsson, J. G.; Svenson, J.; Andersson, H. S.; Nicholls, I. A. Synthesis and Ligand Recognition of Paracetamol Selective Polymers: Semi-Covalent Versus Non-Covalent Molecular Imprinting. *Org. Biomol. Chem.* **2009**, *7*, 3148–3155.
- (38) Sikiti, P.; Msagati, T. A.; Mamba, B. B.; Mishra, A. K. Synthesis and Characterization of Molecularly Imprinted Polymers for the Remediation of PCBs and Dioxins in Aqueous Environments. *J. Environ. Health Sci. Eng.* **2014**, *12*, 82.
- (39) Peppas, N. A.; Khare, A. R. Modern Hydrogel Delivery Systems Preparation, Structure and Diffusional Behavior of Hydrogels in Controlled Release. *Adv. Drug Delivery Rev.* **1993**, *11*, 1–35.
- (40) Nelson, J. R. Determination of Molecular Weight between Crosslinks of Coals from Solvent-Swelling Studies. *Fuel* **1983**, *62*, 112–116.
- (41) Fahmy, R.; Marnane, B.; Bensley, D.; Hollenbeck, R. G. Dissolution Test Development for Complex Veterinary Dosage Forms: Oral Boluses. *AAPS PharmSci.* **2002**, *4*, 137–144.
- (42) Bondesson, L.; Mikkelsen, K. V.; Luo, Y.; Garberg, P.; Ågren, H. Hydrogen Bonding Effects on Infrared and Raman Spectra of Drug Molecules. *Spectrochim. Acta, Part A* **2007**, *66*, 213–224.
- (43) Xia, X.-R.; Monteiro-Riviere, N. A.; Riviere, J. E. An Index for Characterization of Nanomaterials in Biological Systems. *Nat. Nanotechnol.* **2010**, *5*, 671–675.
- (44) Yoshimatsu, K.; Reimhult, K.; Krozer, A.; Mosbach, K.; Sode, K.; Ye, L. Uniform Molecularly Imprinted Microspheres and Nanoparticles Prepared by Precipitation Polymerization: The Control of Particle Size Suitable for Different Analytical Applications. *Anal. Chim. Acta* 2007, 584, 112–121.
- (45) Su, X.; Li, X.; Li, J.; Liu, M.; Lei, F.; Tan, X.; Li, P.; Luo, W. Synthesis and Characterization of Core—Shell Magnetic Molecularly Imprinted Polymers for Solid-Phase Extraction and Determination of Rhodamine B in Food. *Food Chem.* **2015**, *171*, 292–297.
- (46) Lin, H.-Y.; Ho, M.-S.; Lee, M.-H. Instant Formation of Molecularly Imprinted Poly(Ethylene-Co-Vinyl Alcohol)/Quantum Dot Composite Nanoparticles and Their Use in One-Pot Urinalysis. *Biosens. Bioelectron.* **2009**, 25, 579–586.
- (47) Dong, W.; Yan, M.; Liu, Z.; Wu, G.; Li, Y. Effects of Solvents on the Adsorption Selectivity of Molecularly Imprinted Polymers: Molecular Simulation and Experimental Validation. *Sep. Purif. Technol.* **2007**, 53, 183–188.
- (48) Charron, G.; Hühn, D.; Perrier, A.; Cordier, L.; Pickett, C. J.; Nann, T.; Parak, W. J. On the Use of pH Titration to Quantitatively Characterize Colloidal Nanoparticles. *Langmuir* **2012**, *28*, 15141–15149.
- (49) Dong, H.; Du, H.; Qian, X. Theoretical Prediction of pK<sub>a</sub> Values for Methacrylic Acid Oligomers Using Combined Quantum Mechanical and Continuum Solvation Methods. *J. Phys. Chem. A* **2008**, *112*, 12687–12694.
- (50) Park, H.; Robinson, J. R. Mechanisms of Mucoadhesion of Poly (Acrylic Acid) Hydrogels. *Pharm. Res.* **1987**, *04*, 457–464.
- (51) Li, X.; Simmons, R.; Mwongela, S. M. Two-Stage Course-Embedded Determination of Caffeine and Related Compounds by Hplc in Caffeine Containing Food, Beverages and (or) Related Products. J. Lab. Chem. Educ. 2017, 5, 19–25.
- (52) Bernal, V.; Erto, A.; Giraldo, L.; Moreno-Piraján, J. C. Effect of Solution pH on the Adsorption of Paracetamol on Chemically Modified Activated Carbons. *Molecules* **2017**, *22*, 1032.
- (53) Kanani, K.; Gatoulis, S. C.; Voelker, M. Influence of Differing Analgesic Formulations of Aspirin on Pharmacokinetic Parameters. *Pharmaceutics* **2015**, *7*, 188–198.

- (54) Li, Y.; Li, X.; Dong, C.; Qi, J.; Han, X. A Graphene Oxide-Based Molecularly Imprinted Polymer Platform for Detecting Endocrine Disrupting Chemicals. *Carbon* **2010**, *48*, 3427–3433.
- (55) Luo, X.; Dong, R.; Luo, S.; Zhan, Y.; Tu, X.; Yang, L. Preparation of Water-Compatible Molecularly Imprinted Polymers for Caffeine with a Novel Ionic Liquid as a Functional Monomer. *J. Appl. Polym. Sci.* **2013**, *127*, 2884–2890.
- (\$6) Farrington, K.; Magner, E.; Regan, F. Predicting the Performance of Molecularly Imprinted Polymers: Selective Extraction of Caffeine by Molecularly Imprinted Solid Phase Extraction. *Anal. Chim. Acta* **2006**, 566, 60–68.
- (57) Gunasekaran, S.; Sankari, G.; Ponnusamy, S. Vibrational Spectral Investigation on Xanthine and Its Derivatives—Theophylline, Caffeine and Theobromine. *Spectrochim. Acta, Part A* **2005**, *61*, 117–127
- (58) Nanubolu, J. B.; Burley, J. C. Investigating the Recrystallization Behavior of Amorphous Paracetamol by Variable Temperature Raman Studies and Surface Raman Mapping. *Mol. Pharmaceutics* **2012**, *9*, 1544–1558.
- (59) Socrates, G. Infrared and Raman Characteristic Group Frequencies: Tables and Charts, 3rd ed.; John Wiley & Sons Ltd.: West Sussex, England, 2001.
- (60) Zou, Y.; Armstrong, S. R.; Jessop, J. L. P. Apparent Conversion of Adhesive Resin in the Hybrid Layer, Part 1: Identification of an Internal Reference for Raman Spectroscopy and the Effects of Water Storage. J. Biomed. Mater. Res., Part A 2008, 86A, 883–891.
- (61) Zou, Y.; Armstrong, S. R.; Jessop, J. L. P. Quantitative Analysis of Adhesive Resin in the Hybrid Layer Using Raman Spectroscopy. *J. Biomed. Mater. Res., Part A* **2010**, *94A*, 288–297.
- (62) Dirlikov, D.; Koenig, J. L. Infrared Spectra of Poly(Methyl Methacrylate Labeled with Oxygen-18. *Appl. Spectrosc.* **1979**, 33, 551–555.
- (63) Schlücker, S.; Koster, J.; Singh, R. K.; Asthana, B. P. Hydrogen-Bonding between Pyrimidine and Water: A Vibrational Spectroscopic Analysis. *J. Phys. Chem. A* **2007**, *111*, 5185–5191.
- (64) Moskovits, M. Surface-Enhanced Raman Spectroscopy: A Brief Perspective. In *Surface-Enhanced Raman Scattering: Physics and Applications*; Springer: Berlin, 2006; Vol. 103, pp 1–17.
- (65) Ager, J. W.; Veirs, D. K.; Rosenblatt, G. M. Spatially Resolved Raman Studies of Diamond Films Grown by Chemical Vapor Deposition. *Phys. Rev. B: Condens. Matter Mater. Phys.* **1991**, 43, 6491–6499.
- (66) Menéndez, J.; Cardona, M. Temperature Dependence of the First-Order Raman Scattering by Phonons in Si, Ge, and  $\alpha$ -Sn: Anharmonic Effects. *Phys. Rev. B: Condens. Matter Mater. Phys.* **1984**, 29, 2051–2059.
- (67) Kantarovich, K.; Tsarfati, I.; Gheber, L. A.; Haupt, K.; Bar, I. Reading Microdots of a Molecularly Imprinted Polymer by Surface-Enhanced Raman Spectroscopy. *Biosens. Bioelectron.* **2010**, *26*, 809–814.
- (68) McStay, D.; Al-Obaidi, A. H.; Hoskins, R.; Quinn, P. J. Raman Spectroscopy of Molecular Imprinted Polymers. *J. Opt. A: Pure Appl. Opt.* **2005**, *7*, S340–S345.
- (69) Kantarovich, K.; Belmont, A.-S.; Haupt, K.; Bar, I.; Gheber, L. A. Detection of Template Binding to Molecularly Imprinted Polymers by Raman Microspectroscopy. *Appl. Phys. Lett.* **2009**, *94*, 194103.
- (70) Preston, T. C.; Nuruzzaman, M.; Jones, N. D.; Mittler, S. Role of Hydrogen Bonding in the pH-Dependent Aggregation of Colloidal Gold Particles Bearing Solution-Facing Carboxylic Acid Groups. *J. Phys. Chem. C* **2009**, *113*, 14236–14244.
- (71) Torii, H.; Tatsumi, T.; Tasumi, M. Effects of Hydration on the Structure, Vibrational Wavenumbers, Vibrational Force Field and Resonance Raman Intensities of N-Methylacetamide. *J. Raman Spectrosc.* **1998**, 29, 537–546.
- (72) Hanfland, M.; Beister, H.; Syassen, K. Graphite under Pressure: Equation of State and First-Order Raman Modes. *Phys. Rev. B: Condens. Matter Mater. Phys.* **1989**, *39*, 12598–12603.

- (73) Boczar, M.; Wójcik, M. J.; Szczeponek, K.; Jamróz, D.; Ikeda, S. Theoretical Modeling of Infrared Spectra of Salicylaldehyde and Its Deuterated Derivatives. *Int. J. Quantum Chem.* **2002**, *90*, 689–698.
- (74) Kim, H.; Guiochon, G. Adsorption on Molecularly Imprinted Polymers of Structural Analogues of a Template. Single-Component Adsorption Isotherm Data. *Anal. Chem.* **2005**, *77*, 6415–6425.
- (75) Jin, Y.; Row, K. H. Adsorption Isotherm of Ibuprofen on Molecular Imprinted Polymer. *Korean J. Chem. Eng.* **2005**, 22, 264–267
- (76) Jeppu, G. P.; Clement, T. P. A Modified Langmuir-Freundlich Isotherm Model for Simulating pH-Dependent Adsorption Effects. *J. Contam. Hydrol.* **2012**, 129–130, 46–53.
- (77) Klotz, I. M. Ligand-Receptor Energetics: A Guide for the Perplexed; Wiley: New York, 1997.
- (78) Byrne, M. E.; Park, K.; Peppas, N. A. Molecular Imprinting within Hydrogels. *Adv. Drug Delivery Rev.* **2002**, *54*, 149–161.
- (79) Zhang, T.; Liu, F.; Chen, W.; Wang, J.; Li, K. Influence of Intramolecular Hydrogen Bond of Templates on Molecular Recognition of Molecularly Imprinted Polymers. *Anal. Chim. Acta* **2001**, 450, 53–61.
- (80) Matsui, J.; Miyoshi, Y.; Doblhoff-Dier, O.; Takeuchi, T. A Molecularly Imprinted Synthetic Polymer Receptor Selective for Atrazine. *Anal. Chem.* **1995**, *67*, 4404–4408.
- (81) Seong, H.; Lee, H. B.; Park, K. Glucose Binding to Molecular Imprinted Polymers. J. Biomater. Sci., Polym. Ed. 2002, 13, 637–649.
- (82) Hong, J.-M.; Anderson, P. E.; Qian, J.; Martin, C. R. Selectively-Permeable Ultrathin Film Composite Membranes Based on Molecularly-Imprinted Polymers. *Chem. Mater.* **1998**, *10*, 1029–1033.